Wetting of the tarsal adhesive fluid controls underwater adhesion in ladybug beetles: Supplementary information

Pranav Sudersan,† Michael Kappl,† Bat-El Pinchasik,‡ Hans-Jürgen Butt,† and Thomas Endlein†

†*Max Planck Institute for Polymer Research, Ackermannweg 10, 55128 Mainz, Germany*

‡*School of Mechanical Engineering, Tel Aviv University, Tel Aviv-Yafo, Israel*

S1 Simulation method: Single capillary bridge

Capillary force due to a single adhesive fluid or bubble meniscus (termed "capillary bridge") was calculated by performing simulations in Surface Evolver [1], similar to the method described by De Souza et al. [2]. A simple cubic geometry, mimicking the capillary bridge, of constant volume, V, was defined as the initial condition with an interfacial tension, γ, with the surrounding medium. Interfacial tension of the capillary bridge with the substrate is given by $\gamma \cos\theta$, where θ is the corresponding contact angle inside the bridge. For the case of a bubble meniscus, θ is defined w.r.t. the surrounding water, since θ can also directly characterise the substrate wettability. The capillary bridge spans a gap distance d between the top face and the substrate. The boundary conditions were set corresponding to a pinned contact line of diameter D on the top face and constant interfacial tension with the substrate on the bottom. All lengths were normalised relative to length $s = (3V/4\pi)^{1/3}$. An appropriate geometry refinement routine was chosen to evolve the capillary bridge shape to its minimum energy state. The normalised total capillary force, $\hat{f} = f/\gamma s$, is the sum of the Laplace pressure and surface tension contributions , where:

$$f = f_{laplace} + f_{surface\,tension} = \Delta P_{laplace} A_{bottom} + 2\pi R_{bottom} \gamma \sin\theta \tag{S1}$$

Here, $\Delta P_{laplace}$ is the Laplace pressure of the equilibrium capillary bridge, A_{bottom} is the contact area of the capillary bridge with the substrate at bottom and R_{bottom} is the corresponding radius of contact, all obtained from the simulation output for the equilibrium surface.

The gap distance d was varied stepwise and the capillary force was calculated each time to obtain force-distance curves for a particular choice of D and θ.

S2 Substrate characterization

The surface chemistry of untreated glass (hydrophilic) and PFOTS-coated glass (hydrophobic) were characterized using dynamic contact angle measurements (Table S1).

Table S1: Dynamic contact angles (Mean ± SD, n = 3) of Milli-Q water and n-hexadecane on the different test substrates.

Substrate	Liquid	θ_A	θ_R
Glass	Water	63±5°	20±2°
	n-Hexadecane	<10°	<10°
PFOTS	Water	122±1°	93±2°
	n-Hexadecane	88±2°	56±5°

S3 Statistical comparison

Two-way ANOVA test showed a significant effect of the *Contact mode* (p=0.001, F=9.596, degrees of freedom=2) and *Substrate* (p<0.001, F=36.231, degrees of freedom=1) categories on the single leg adhesion force measurements of the ladybug beetle (*Coccinella septempuctata*). Signifanct interaction between the above two categories was seen (p=0.001, F=10.551, degrees of freedom=2). Post-hoc analysis results are shown below (Table S2). The uncorrected p-values and Common Language Effect Size (CLES) were obtained from pair-wise Student t-test between A and B while keeping the third parameter fixed (degrees of freedom=8 for each pair). p-values showing statistically significant difference between A and B are in boldface. CLES represents the statistical proportion of samples under A with higher adhesion than under B. The condition for statistical significance is based on the Bonferroni-corrected critical p-value of 0.008.

Table S2: Post-hoc t-test results for each combination of contact mode and substrate

Fixed variable	A	B	T	p-value	CLES
In air	PFOTS	Glass	-0.053	0.959	0.48
Underwater: bubble	PFOTS	Glass	3.292	0.011	0.96
Underwater: no bubble	PFOTS	Glass	10.044	0.0	1.0
PFOTS	In air	Underwater: bubble	0.133	0.897	0.48
PFOTS	In air	Underwater: no bubble	-0.224	0.828	0.48
PFOTS	Underwater: bubble	Underwater: no bubble	-0.37	0.721	0.44
Glass	In air	Underwater: bubble	4.688	0.002	1.0
Glass	In air	Underwater: no bubble	11.341	0.0	1.0
Glass	Underwater: bubble	Underwater: no bubble	2.086	0.07	0.84

S4 Capillary force due to an air bubble

Capillary force of a single air bubble against a PFOTS-coated glass surface are compared for two different volumes (Figure S1). The volumes correspond to the expected range for the case of the trapped air bubble in a ladybug's pad. Here, the bubble was pinned to a micropatterned PDMS substrate on the top. Approach-retract tests were performed at

62.5 µm s^{-1} speed. The maximum adhesion force of any of the bubble never exceeds 50 µN, significantly lower than the beetle's underwater adhesion to the same substrate (> 400 µN). Thus, the bubble's contribution to adhesion in the "*underwater: bubble*" contact of a ladybug's pad should be negligible. Example measurement video is included in the supplementary data (Movie3).

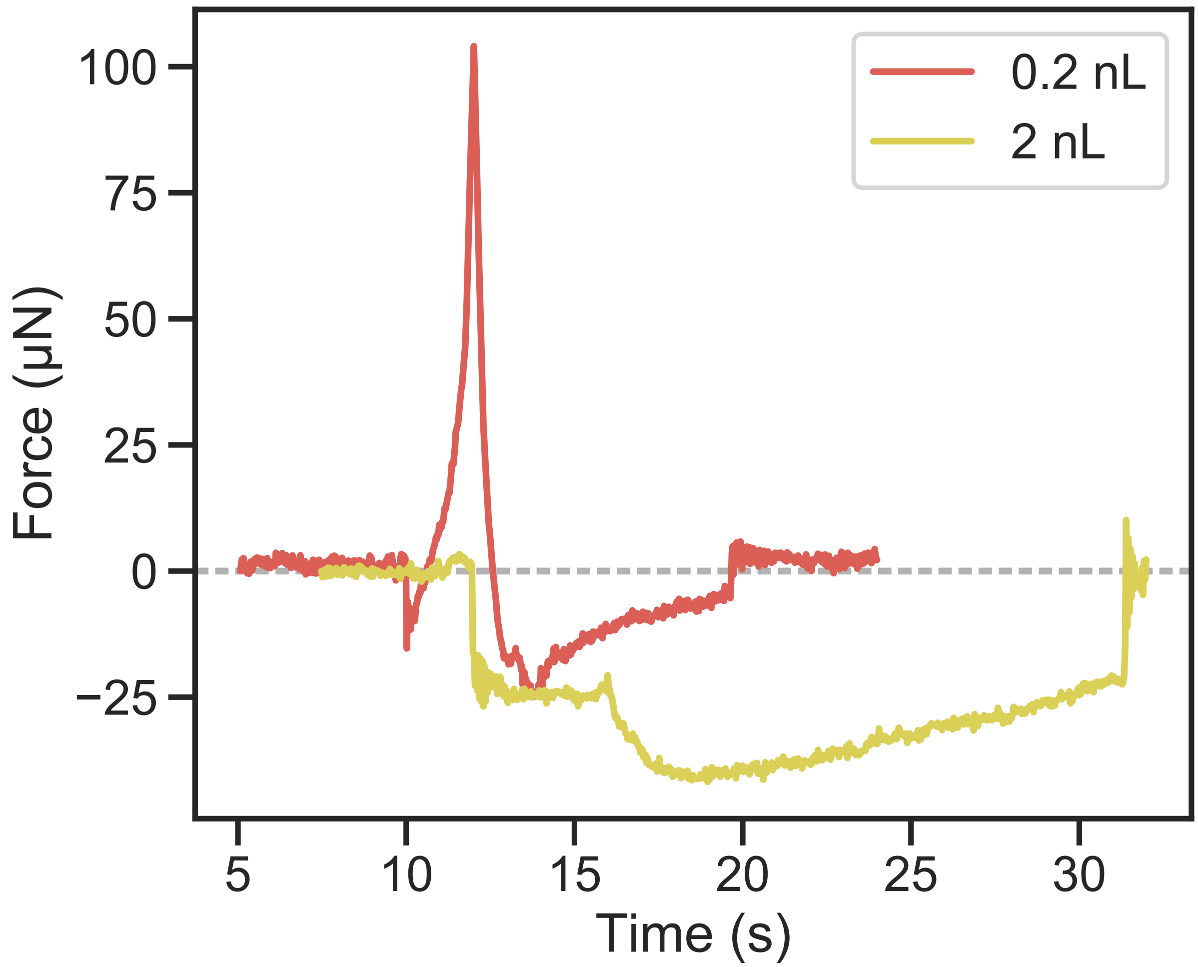

Figure S1: Capillary force of the pinned bubble against a PFOTS-coated glass surface

S5 Capillary bridge model: Sensitivity analysis

Sensitivity analysis was performed using the one-at-a-time (OAT) method. Dimensionless model parameters were initially set to correspond to the ladybug's case, as given by, contact area fraction ($\alpha = 0.1$), pad to hair diameter ratio ($D_p/D_h = 50$), hair aspect ratio ($L/D_h = 10$), water surface tension ratio ($\gamma_{wa}/\gamma_{fa} = 3$), tarsal fluid-water interfacial tension ratio ($\gamma_{fw}/\gamma_{fa} = 2$), tarsal fluid size parameter ($\phi_f = 2$), bubble size parameter ($\phi_b = 1.6$). Substrate contact angles were kept fixed (same as in main text). Each parameter was varied within a particular range, one at a time, and the corresponding adhesion forces *in air* ($\mathrm{F_a}$), *underwater: no bubble* ($\mathrm{F_w}$) and *underwater: bubble* ($\mathrm{F_b}$) were calculated. Linear least square regression was performed to quantify the relative change in adhesion for each contact mode with respect to the varied parameter. Here, $\mathrm{F_w}/\mathrm{F_a}$ and $\mathrm{F_b}/\mathrm{F_a}$ were taken to be the model output. Slope and R^2 values for each case are reported below (Table S3).

Table S3: Sensitivity analysis

Parameter	**Range**	**Substrate**	$\mathbf{F_w/F_a}$		$\mathbf{F_b/F_a}$	
			slope	$\mathbf{R^2}$	**slope**	$\mathbf{R^2}$
α	0.05, 0.3	Hydrophilic	3.03E-18	1.52E-03	2.30E-01	7.72E-01
		Hydrophobic	-9.69E-17	3.03E-03	-9.40E-01	7.72E-01
D_p/D_h	30.0, 60.0	Hydrophilic	-8.83E-20	1.48E-01	1.28E-02	9.73E-01
		Hydrophobic	-5.65E-18	1.48E-01	-1.51E-02	9.82E-01
L/D_h	8.0, 15.0	Hydrophilic	0.00E+00	0.00E+00	-5.27E-02	9.11E-01
		Hydrophobic	0.00E+00	0.00E+00	5.41E-02	8.66E-01
γ_{wa}/γ_{fa}	2.5, 3.5	Hydrophilic	-2.01E-01	8.57E-01	-2.43E-01	9.43E-01
		Hydrophobic	4.11E-02	1.00E+00	6.87E-02	1.00E+00
γ_{fw}/γ_{fa}	1.5, 2.5	Hydrophilic	2.01E-01	8.62E-01	1.90E-01	8.94E-01
		Hydrophobic	5.56E-01	1.00E+00	1.57E-01	1.00E+00
ϕ_f	1.7, 2.2	Hydrophilic	1.29E-02	4.52E-01	6.18E-02	7.94E-02
		Hydrophobic	7.67E-02	9.84E-01	-3.06E-01	9.66E-01
ϕ_b	1.2, 1.8	Hydrophilic	0.00E+00	0.00E+00	-1.14E+00	8.85E-01
		Hydrophobic	0.00E+00	0.00E+00	1.46E+00	9.78E-01

S6 Supplementary video files

Movie1

Adhesion test recordings showing the three contact modes: *in air*, *underwater: bubble* and *underwater: no bubble* on a hydrophobic PFOTS-coated glass substrate. The two top panels of the video show the synchronous raw bottom-view and side-view recordings of the pad making contact with the substrate. The lower-left panel shows contact area extraction of the hairs with the surface via image processing and lower-right panel shows the corresponding temporal contact force and area data plot, with the data cursor synchronized with the other panels.

Movie2

Adhesion test recording corresponding to the case of *bad contact*, which occurred underwater on the PFOTS-coated glass substrate

Movie3

Adhesion test recording of an air bubble (2nL volume) pinned to a microstructured PDMS on the top and making contact with a smooth PFOTS-coated glass substrate on the bottom.

References

(1) Brakke, K. A. The surface evolver. *Experiment. Math.* **1992**, *1*, 141–165.

(2) De Souza, E. J.; Brinkmann, M.; Mohrdieck, C.; Arzt, E. Enhancement of Capillary Forces by Multiple Liquid Bridges. *Langmuir* **2008**, *24*, 8813–8820.